Proceedings of ASME Turbo Expo 2011
GT2011
June 6-10, 2011, Vancouver, British Columbia, Canada

GT2011-45417

PREDICTIONS OF EFFUSION COOLING WITH CONJUGATE HEAT TRANSFER

Habeeb Idowu Oguntade[2], Gordon E. Andrews[1], Alan Burns[2], Derek Ingham[2] and Mohammed Pourkashanian[1, 2]

[1]Energy and Resources Research Institute and [2]the Centre for Computational Fluid Dynamics,
School of Process, Environment and Materials Engineering
University of Leeds, UK.
Email: mnhio@leeds.ac.uk

ABSTRACT

This work involves CFD conjugate heat transfer modelling of the geometrical design influence on effusion cooling. Experimental data was modelled for the overall effusion film cooling effectiveness using Nimonic 75 walls with imbedded thermocouples. The Fluent CFD code was used to investigate the experimental configuration for a 10×10 square array of holes with a 90^o injection angle. In the computational predictions, 10000ppm of methane tracer gas was added to the coolant and the concentration at the wall allowed the adiabatic cooling effectiveness of the effusion film cooling to be predicted separately from the overall wall cooling effectiveness. The predicted overall cooling effectiveness results show that the wall was locally at a uniform temperature, but the axial development of the cooling film does result in a gradual reduction of the wall temperature with axial distance. The predictions show that the heating of the coolant by the hot wall was equally split between the hole approach flow on the backside of the wall and inside the film cooling holes. This heating changed the conditions in the film cooling layer from those of the equivalent adiabatic wall. There was good agreement between the conjugate heat transfer predictions of the overall cooling effectiveness with the experimental data.

INTRODUCTION

In modern gas turbines, the operating temperatures of the turbine hot-sections have far surpassed the permissible material temperatures of the parts that envelop the hot-gas-path. Thus, efficient cooling of the combustor and turbine blades is essential to the operation of modern gas turbines to give these components a durable life span. Moreover, established trends [1] have shown that the next generation of gas turbines will continue to have increasing turbine inlet temperatures with the same or lower mass of air used for cooling. Unless there is a dramatic breakthrough from the metallurgists, by providing a much higher temperature alloy material, the provision of better cooling remains the only viable option to providing a reasonable service life for the turbines hot components.

An ideal cooling system would be one that offers an evenly cooled wall surface with the minimum coolant air requirement. The closest to the ideal cooling system is transpiration cooling [2-6]. However, this technique has mechanical disadvantages, such as structural strength, oxidation and blockages of the small flow passages [2-6]. Effusion cooling is a simpler version of transpiration cooling technique, free from the mechanical problems associated with the transpiration cooling. Effusion cooling has the potential for high cooling performance with reduced cooling air mass flow requirement, which is essential for high cycle efficiency and for combustor low NOx designs [7].

Film and effusion cooling has three main components: the film cooling, back side convective heat transfer and internal passage convective heat transfer. Most of the experimental and computational studies on film and effusion cooling [8-15] have concentrated on the measurement of the adiabatic film cooling effectiveness with the wall temperatures predicted using separate measurements of the internal passage and backside convective heat transfer coefficients. However, there is growing interest in the measurements of the overall heat transfer in real metal blades and combustor walls, as the interaction of the heat exchange between the solid wall and the fluid flow are not included when the adiabatic film cooling effectiveness is measured alone. The heat transfer in the wall changes the DR at the hole outlet from that based on the supply conditions.

Esgar [6] investigated the relative potentials of convection, transpiration and effusion film cooling. The measured temperature rise of the coolant through an effusion cooled wall was about 250K for a primary and secondary flow temperature of 1800K and 811K, respectively. Thus the exiting jet temperature would be 1061K and the density ratio would be reduced from 2.2 to 1.7. Computational studies that address the adiabatic film cooling and the solid wall conduction heat transfer, as well as the internal passage backside convection heat transfer are known as conjugate heat transfer predictions. Experimental studies with metal walls and hot crossflow measure a cooling effectiveness usually referred to as the overall cooling effectiveness, which distinguishes it from the adiabatic film cooling effectiveness.

To the best our knowledge there are no other effusion cooling studies on a conjugate heat transfer basis that have attempted to separate the overall from adiabatic cooling effectiveness, except for those by Andrews and his co-workers [18-29]. They extensively studied effusion cooling and have produced an experimental data set for the overall cooling effectiveness of the effusion film cooling. The present work computationally models one of their experimental data sets and future work will examine the range of geometrical variables studied in the experimental work. In addition to the overall cooling effectiveness measurements, Andrews and co-workers have determined the heat transfer coefficients for the internal wall cooling of effusion cooling geometries [26-29].

Backside heat transfer can be enhanced in effusion cooling if it is combined with impingement cooling into an impingement/effusion cooled wall. Andrews and co-workers [30-34] have investigated the geometries used in their effusion cooled work in combination with impingement cooling. These configurations had the main pressure loss at the impingement wall and a low pressure loss and low blowing rates at the effusion wall. Future work is intended to apply the present conjugate heat transfer predictions to these more complex impingement/effusion cooling situations.

Jung et al [35, 36] have recently investigated impingement/effusion cooling in similar configurations to that of Andrews and co-workers, with measurements of the overall cooling effectiveness. Their effusion and impingement plates have respective 30^0 and 90^0 injection angles to the stream wise direction. They showed that the total cooling effectiveness data of their staggered holes arrangement was generally better than their previous inline hole arrangement total cooling effectiveness data. Crawford et al. [37] experimentally investigated the heat transfer over the turbulent boundary layer of an effusion cooled flat surface. They found that the 30^0 inclined hole injection has lower jet penetration than the normal injection. Jeromin et al. [38] presented a numerical prediction of the conjugate heat transfer of an effusion cooled wall with staggered holes array. The predictions of their heat transfer coefficients results demonstrated good agreement with the experimental data at low blowing ratio.

Harrington et al. [39] investigated the effects of turbulence on the effusion film cooling performance and the accuracy of a superposition prediction of effusion cooling with a single row of holes. Relatively short normal injection holes, similar to some of those used by Andrews and co-worker [19, 20], were used in their studies. They found that high mainstream turbulence reduced film cooling performance more at low blowing ratios than at high blowing ratios with jet separation. The high mainstream turbulence helped in the returning of some of the penetrating coolant jet back to the surface of the test wall. Also, they found that the superposition model did not account for the row to row coolant jet interactions. Gustafsson et al. [40] carried out a parametric study of the temperature distribution on an effusion-cooled wall with different temperature and velocity ratios, hole pitch, injection angle and thermal conductivity ratios between the effusion and plenum. They found that changes in the amount of coolant air had a small effect on the surface temperature distribution of a sparsely spaced effusion film cooling holes. Also, Scrittore et al. [41] investigated the flowfield of effusion film cooling and demonstrated that sparsely spaced effusion cooling holes had a unique scalable velocity profile.

The present study uses a numerical simulation based on the control volume method to model one of the experimental data sets of Andrews and co-workers. This numerical study aims to reveal more information that will complement the experimental data for a better understanding of the aerodynamic and conjugate heat transfer process of the effusion cooling as required for improved effusion cooling design parameters.

EXPERIMENTAL FACILITY

The experimental effusion test plate and duct wall that was modelled was made from a Nimonic-75 alloy and ceramic, respectively. The test plate had a 10 × 10 square array of holes and was 152.4mm square in its exposed surface area [18]. The experimental test rigs consisted of an insulated coolant air plenum chamber mounted in the top wall of the 76mm deep by 152.4mm wide duct [17-21]. A 152.4mm square test plate with an array of equispaced and equal diameter holes formed the bottom part of the plenum chamber. The test plate was bolted to the plenum chamber. Internally, the plenum chamber was insulated to prevent heat loss from the coolant to the plenum wall. The test walls used the same material and thickness as large heavy duty gas turbine combustor wall. Hence the low Biot numbers (<0.1) were representative of combustor walls. However, the wall conduction is similar for turbine blades as the alloys used have similar thermal conductivities to that of Nimonic 75. Wall thickness are lower in turbine blades so lower internal hole heat transfer will occur, but this is a small effect as the heat transfer is concentrated in the inlet region of the holes.

The initial test rig had a high temperature ceramic wall (Rig1) which proved satisfactory for the low temperature test conditions, with the hot gas temperature less than 900K. However, at elevated combustion temperatures, the ceramic duct wall glowed red hot and produced a very high radiation heat interchange between the duct wall and the effusion test plate. Avoidance of this radiation heat interchange led to the construction of the air cooled steel duct wall (Rig 2) used in the later studies [17, 18]. The duct cooling air flow for the Rig 2 was varied to achieve the same duct wall temperature as for the centre of the effusion test wall. The authors [17, 18] found that Rig 1 and Rig 2 yielded the same temperature measurements of the test plate for the low temperature test conditions with the hot gas temperature less than 900K.

As for the low temperature test conditions, the hot gas temperature was generated using an upstream propane combustor, which was operated very lean to generate the desired hot gas temperature. This was mounted upstream of the flame stabiliser or turbulence grid plate. The overall cooling effectiveness data was obtained from the effusion wall temperature measurements using imbedded Type K mineral insulated thermocouples at five equispaced locations, in the hottest position of the mid-span between the centre rows of holes. The thermocouples were spaced 25.4mm apart and the locations relative to the coolant holes are illustrated in Fig 1(b). The first effusion wall imbedded thermocouple was located at 25.4mm axial distance downstream of the LE of the test plate, the fifth thermocouple was located 127mm axial distance downstream of the LE effusion plate.

The dimensionless temperatures of the hot gas adjacent to the test plate surface was related to the adiabatic cooling effectiveness and this was measured by traversing a bare bead thermocouple positioned at the centre of the duct. The traversing thermocouple had a low voltage electric circuit that would indicate contact of the thermocouple with the test wall. The traverse thermocouple stepper motor was then moved slightly to break the contact with the test plate and the gas temperature at that point was used to obtain the pseudo-adiabatic cooling effectiveness. However, it is important to note that this is different from the conventional way of obtaining an adiabatic cooling effectiveness from a high thermal conductivity wall [10]. The CFD predictions of this near wall temperature will be compared with the experimental data. The comprehensive description of the experimental facilities and employed heat transfer procedure are as documented by the authors [17, 18].

The application of the experimental data was to combustor wall cooling, but the results have application to turbine blade cooling. The original data was aimed at a design procedure for combustor full coverage effusion cooling and for impingement/effusion cooling and has been in use for several years by industry. The weakness of the data set for CFD validation is that the velocity profile and turbulence level of the crossflow were not measured, but were set to be similar to practical combustors by operating the crossflow pressure loss across the grid plate type flame stabiliser at 4% of the upstream pressure, at the crossflow mean velocity of 27 m/s.

Table 1 The geometrical and flow conditions

D	3.27mm	T_c	300K
X/D	4.66	T_g	750K
X	15.24mm	u_g	27m/s
N	4306/m^2	Tu_g	10%
L	6.35	DR	2.5
α	90^0	G	0.088-1.47kg/sm^2

COMPUTATIONAL PROCEDURE

The computational procedures and the justification for their use are those set out by the authors [17] for the modelling of a single row film cooling holes, using the classic adiabatic cooling effectiveness experimental data [10, 12]. The computational domain consisted of the plenum coolant air, the duct crossflow, the test plate and the top solid wall of the duct as shown in Figs. 1 and 2. Nimonic-75 alloy and ceramic are respectively used as the test plate and the top solid wall of the duct to match that used in the experiment.

The experimental data were for the centreline between the effusion cooling holes, where edge wall effects were negligible. Thus, to reduce computational requirement, only half of the centre row of holes was modelled (as shown by the dotted line in Fig. 1b) and symmetry boundary conditions were specified at the centreline and mid-span plane of the holes. The duct inlet boundary conditions and the plenum inlet temperature remained fixed while the plenum inlet coolant mass flow rate per surface area, G kg/sm^2, was varied and matched that used in the experiment as shown in Table 1. A separate computation was performed for each G and 13 computations for the same geometry were carried out in order to predict the influence of G on the overall cooling effectiveness.

The overall three-dimensional computational domain in length, height, and width were 791.7mm, 228.6mm and 7.62mm, respectively. Hexahedral grid was used for the whole computational domain. The momentum, energy, turbulence kinetic energy and dissipation equations were discretized with a second-order upwind scheme and solved using the realizable k-ε model with enhanced wall treatment in the Fluent code. The enhanced wall treatment is a near-wall modelling approach that combines a 2-layer model with the enhanced wall function. In this approach, a new wall formulation is developed to blend the log and linear laws-of-the-wall in order to resolve the flow gradients in the viscosity affected near-wall region down to the wall. Thus, sufficiently fine meshes are clustered around the wall while coarse meshes are used away from the wall.

The grid size was initially 1.08million and after the final adaption, it increased to approximately 2.5million cells for all the G values investigated. The grid adaption was automatically undertaken in the regions of high gradients of the pressure, velocity, temperature and immediate wall region. This adaption ceased when the results no longer changed with the grid refinement, and then the results were taken to be grid independent. The initial value of the y+ was approximately 5 and final y+ values after the final adaption was approximately 1.5. The computational grid before adaption for the modelled test plate geometry is shown in Fig. 2. The convergence criteria for all residuals were set to be 10^{-5}, except for the energy residual which remained at the default value of 10^{-6}. The net mass flow rate imbalance for all simulations was less than 0.002%. The present computations were for the low temperature test conditions and were modelled without radiation from the hot crossflow and between the duct walls. The justification for this was the low crossflow temperature and the soot free upstream propane combustion system.
In the experimental set-up, a coolant air distributor was positioned about 300mm away from the test plate to feed the holes with a uniform velocity distribution. Also, a turbulence grid representing a low NOx combustor was positioned about 300mm upstream of the test plate LE. This has been computationally considered with the assumption of a uniform velocity profile and a moderate 10% turbulence level at the duct and plenum inlets. In the present study, the computation was simplified by using hot air in the duct flow as the thermodynamic properties were close to those of the very lean propane fuelled combustion flame used in the experiment.

The heat and mass transfer analogy was employed to predict the adiabatic cooling effectiveness. This was done by adding a 1% methane tracer gas to the plenum coolant air supply which did not significantly change the density of the coolant. The mass fraction of the methane at the wall was used to compute the adiabatic cooling effectiveness as follows.

$$\eta_{ad} = \frac{C_g - C_w}{C_g - C_c} = \frac{C_w}{C_c} \qquad (1)$$

This technique has previously been used experimentally by Pederson et al. [11] and computationally by Oguntade et al. [15]. This enabled the adiabatic cooling effectiveness of the effusion cooled wall to be predicted separately from the overall cooling effectiveness.

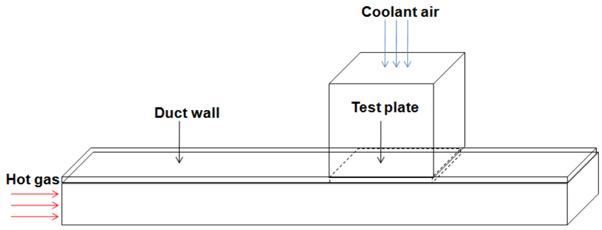

(a) The rig test section area

* - Embedded thermocouples   o - Film cooling holes

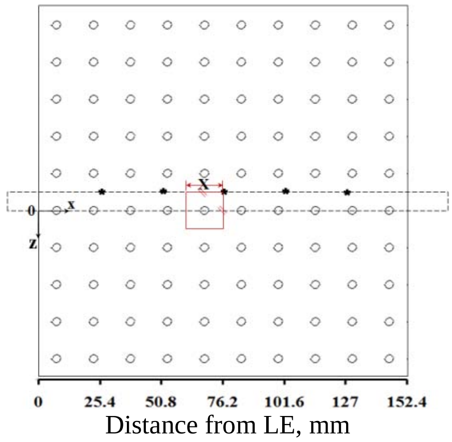

(b)Test plate with the 10×10 array of holes, thermocouple arrangements and computational domain

Fig. 1 Schematic of the test rig

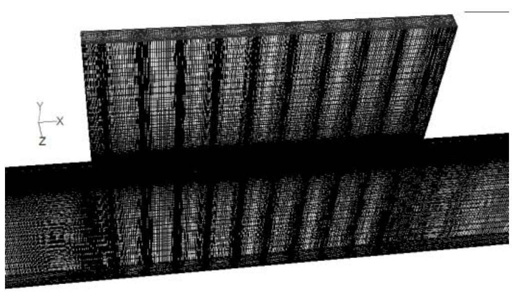

Fig. 2 The computational grid before adaption

RESULTS AND DISCUSSION

The variation of the overall cooling effectiveness with axial distance for the mass flow rate, G = 0.35kg/sm^2 or blowing ratio, M = 0.78 is shown in Fig. 3. The conjugate heat transfer prediction of the overall cooling effectiveness was in good agreement with the experimental data trends with axial distance. The overall cooling effectiveness experimental results were for the hottest region of the test plate at the mid-span between rows of holes. The predictions were slightly higher in the downstream region of the test wall, but in excellent agreement at the first measurement point, 25mm from the leading edge.

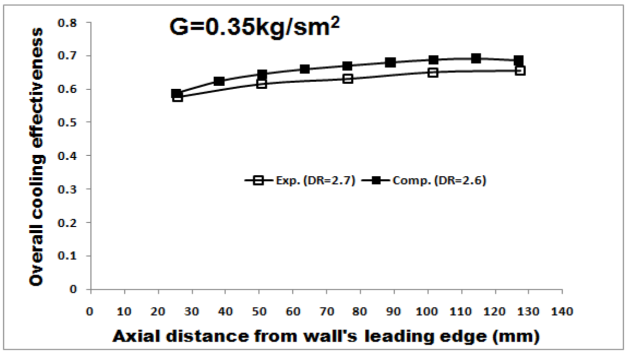

Fig. 3 Variation of overall cooling effectiveness with axial distance for G=0.35 kg/sm^2 and M=0.78

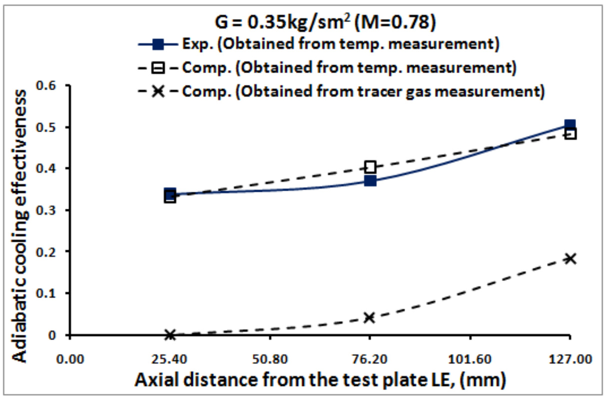

Fig. 4 Variation of adiabatic cooling effectiveness with axial distance for G=0.35 kg/sm^2 and M=0.78

Figure 4 shows the measured and predicted variation of the η_{ad} with axial distance. The predicted η_{ad} was computed from equation (1) in addition to the same way it was obtained in the experiment from the hot gas temperature measurements adjacent to the test plate. The predicted η_{ad} result, based on the hot gas temperature measurements, is obtained at a vertical distance of 0.25mm away from the test plate hot surface and it is in good agreement with the experimental data. The predictions surmised that this measurement was taking at a 0.25mm vertical distance adjacent to the wall. As this was the closest result to the experimental data among those that were taken between the 0.25mm - 1.5mm distance away from the wall. However, the value of η_{ad} obtained from wall adjacent hot temperature measurements is different from that obtained from the tracer gas prediction. The large variation in the η_{ad} results shown in Fig. 4, due to the techniques used indicates that the actual η_{ad} was not measured in the experiment and that the film cooling layer was significantly heated by the coolant passing through the wall and in contact with the wall on the hot-side. Nevertheless, this difference in the predicted results shown in Fig. 4 should possibly be less. This is because several computational studies of the single row of holes [10-13] have shown that the experimental η_{ad} data is under-predicted at the mid-span region and over-predicted at the hole-centreline region. The over-prediction and under-prediction could be partly due to the inadequacy of the RANS model to accurately account for the coherent turbulent structures.

Figure 5 shows the predictions of the η_{ad} and η_{ov} surface distributions for a coolant mass flow rate, G of 0.35kg/sm^2 (M = 0.78). The predicted spread of the methane tracer gas across the wall surface shown in Fig. 5(a) indicates that the spatial coverage of the coolant over the entire wall surface of the plate only occurred after the fifth row of holes. Prior to this, the centreline between the holes had a zero methane concentration. At the trailing edge the coolant spreads across the entire surface of the wall. Also, a steep variation of η_{ad} is shown in Fig. 5. This implies that it is not enough to characterise the cooling performance at a single point. However, the objective of the experiments was to demonstrate the trends with coolant mass flow and the changes that occurred for the same location as the effusion hole geometry was changed.

The validity of the η_{ad} predictions with the tracer gas is based on the previous work for the single row of film cooling holes, where the predictions had reasonable good agreement with the experimental data [15]. Thus it is considered that the present surface distribution predictions of η_{ad} in the presence of active wall heat transfer were reliable.

The predicted η_{ov} contour, shown in Fig. 5(b), indicates that the test plate was relatively evenly cooled after the first row of holes, in spite of the evidently large spatial gradients of the η_{ad} contour. This demonstrates the strong influence of thermal conduction in the metal wall in averaging the effect of the film and internal hole cooling. Also, Gustafsson et al. [40] reported smoother surface temperature profiles for their higher thermal conductivity effusion test plate as well as a lower temperature upstream of the first row of holes.

Figure 6 shows the normalised tracer gas concentration and temperature distributions transverse to the flow and normal to the wall, at the planes 25.4mm. 76.2mm and 127mm from the leading edge (LE) of the test plate for G = 0.35kg/sm^2. The results have been normalised in the same way as the cooling effectiveness is defined. The concentration of the tracer gas in Fig. 6(a) shows the visualization of the coolant jet mixing with the cross flow. This shows that at this relatively low blowing ratio, the 90^o coolant jets are deflected by the crossflow and coalesce to the test plate surface. The coolant jet velocity is given by

$$u_j = \frac{1.27G(X/D)^2}{\rho_j} \quad (2)$$

for a value of n of 4306/m^2 and D of 3.27mm. The jet velocity for a G of 0.35 kg/sm^2 was 8.23 m/s and this was much less than the mean crossflow velocity of 27 m/s. Thus, there would be relatively little penetration of the coolant jet into the crossflow, as has been predicted, compared to the Fig 7 which has a high jet penetration. At the 25mm plane from the LE of the test plate, the dimensionless tracer gas concentration contours, shown in Fig. 6(a), indicate that the spreading of the coolant jet did not reach the midspan. Thus, there was no film cooling protection for the midspan of the wall surface.

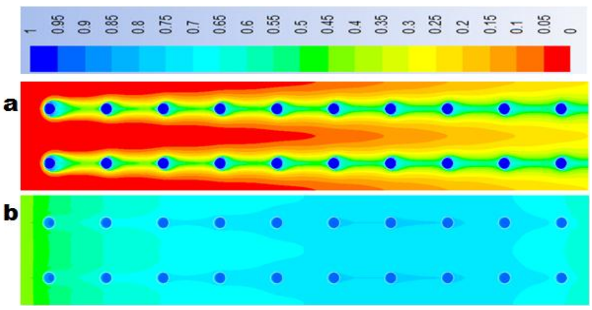

Fig. 5 Contours of the plate spatial effectiveness for G = 0.35kg/sm^2 and M=0.78, (a) adiabatic cooling effectiveness and (b) overall cooling effectiveness

A comparison of the dimensionless temperature contours with the tracer gas concentration contours for the same 25mm plane from the LE in Fig. 6 shows a significant impact of the wall heat transfer on the thermal boundary layer. Cooling of the midspan region by heat extraction by the internal wall heat transfer is demonstrated in Fig. 6(b). At the 127mm plane from the LE, the coolant jet has spread laterally and there is a major impact on the thermal boundary layer by the heat extraction through the wall.

Fig. 7 shows the contours of the dimensionless tracer gas concentration and temperature distribution for a coolant mass flow rate, G of 1.08 kg/sm^2 with a corresponding M of 2.4. The blowing ratio, M = 2.4 is a typical scenario of a lifted jet. The jet velocity for a G of 1.08 kg/sm^2 was 24 m/s and this was about the same as the cross flow velocity of 27 m/s. Fig. 7 shows that the coolant jet lifted completely away from the test plate surface. Comparison of the dimensionless tracer gas concentration distributions between Fig. 6 and Fig. 7 shows no improvement in the adiabatic cooling effectiveness with an increase in the coolant mass flow rate at the 25mm plane from the LE. In fact it is evident that the jet lifted off completely from test plate. However, at the 127mm plane, the adiabatic cooling effectiveness increased with an increase in the coolant mass flow rate, due to the strong mixing between the jet and the cross flow which improves the film cooling potential at the wall surface.

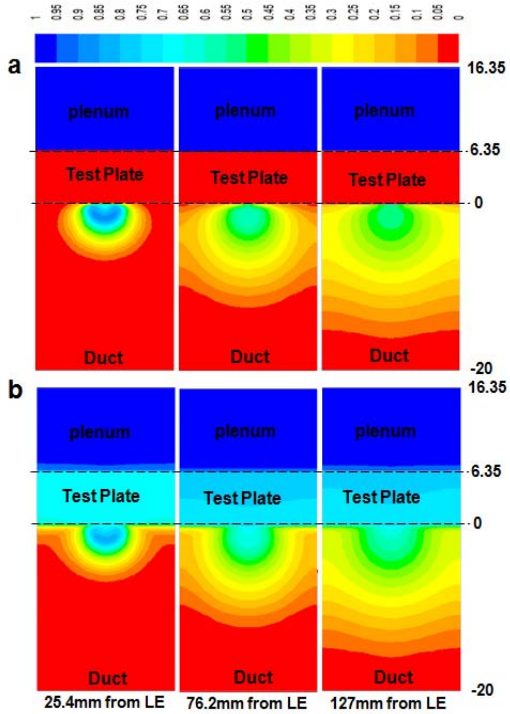

Fig. 6 Contours of the (a) dimensionless tracer gas concentration, and (b) dimensionless temperature distributions for G=0.35kg/sm^2 (M = 0.78)

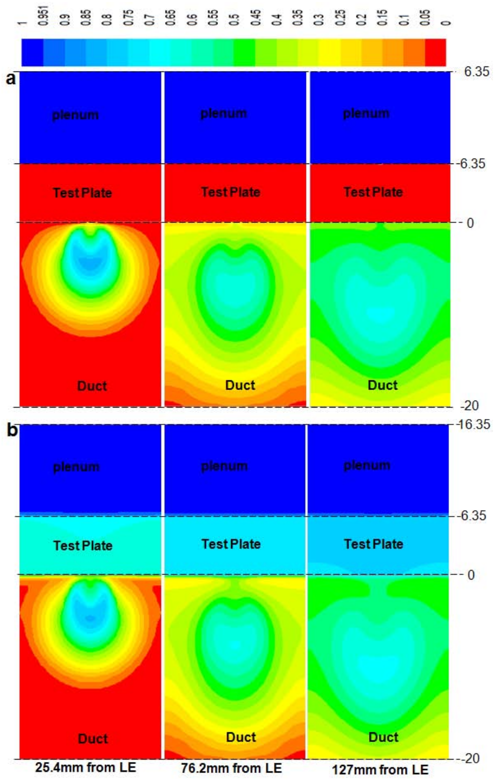

Fig. 7 Contours of the (a) dimensionless tracer gas concentration, and (b) dimensionless temperature distributions for G=1.08kg/sm^2 (M=2.4)

The dimensionless temperature pick-up by the plenum coolant air en-route to the hot wall surface is shown in Fig. 8. The heat transfer on the hole approach surface area is shown separately to that inside the individual hole. It should be noted that the square with length X in Fig. 1 depicts the individual hole approach surface area, A_x. The predictions show that the two heat transfer modes at the centre of the test plate are of similar magnitude in the overall wall heat transfer. However, at the leading and trailing edge regions of the test plate, the individual hole approach surface area heat transfer was shown to be higher than that of the individual internal hole surface area heat transfer mode. Andrews et al. [28] reported that the hole approach convective heat transfer was the dominant heat transfer mode. Also, shown in Fig. 8 is the plot of the overall heating within the wall which was due to the combined heat pick-up by the coolant jet on the hole approach surface area and inside individual holes.

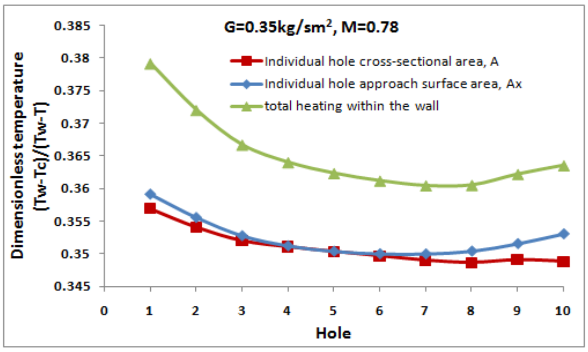

Fig. 8 Dimensionless temperature pick-up at the individual hole approach surface, Ax and internal hole cross-section area, A

Influence of G and M on the Cooling Effectiveness

Figure 9 shows the η_{ov} and η_{ad} as a function of coolant mass flow rate, G and blowing ratio, M (top scale). These results are for the 127mm axial distance downstream of the test plate LE. The predicted η_{ad} results were obtained based on the two different techniques discussed above in relation to Fig. 4. The experimental overall and pseudo-adiabatic cooling effectiveness data increased steeply with increase in G from 0.088-0.3kg/sm^2 and slowly with increase of G from 0.3-1.47kg/sm^2. This was because the effusion film was attached to the wall at the low range of G and detached at the high range of G. However, the predictions showed much less dependence on G and M for the overall cooling effectiveness, but a large dependence on the adiabatic cooling effectiveness.

The predicted values of overall cooling effectiveness were in reasonable agreement with the measurements, except in the leading edge region, which was overpredicted. The same was found for the temperature close to the wall at the midpoint position. This was predicted to give a cooling effectiveness that was too high in the leading edge region.

For the effusion wall design investigated, both the predicted and measured results indicate that there was relatively little improvement in the η_{ov} with the increase in coolant mass flow rate above 0.35kg/sm^2 (M = 0.78). However, the predicted η_{ov} results plateaus more than the experiments data for the same values of G higher than 0.35kg/sm^2. Any increases in G which does not significantly increase the cooling effectiveness

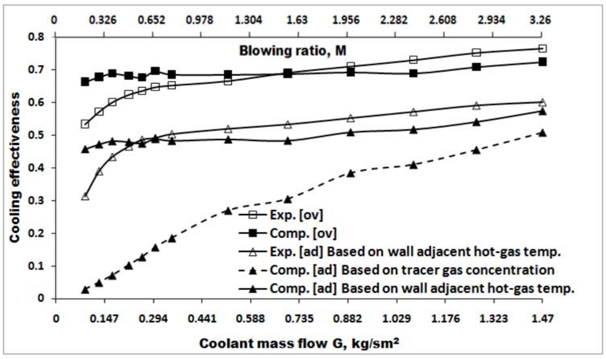

Fig. 9 influence of G and M on cooling effectiveness at the 127mm axial distance downstream of the test plate LE

may not warrant the penalty that will be incurred due to this increase usage of the coolant air. In other words, the predicted and measured η_{ov} results of this effusion wall design suggest that there is little justification for the use of a coolant mass flow, G > 0.35kg/sm^2. This is because once the coolant jets are lifted the act as local turbulent mixing with the crossflow and entrain hot gases close to the wall in the interjet region.

Transverse Spread of the Effusion Film Cooling

Figures 10 and 11 show the predicted contours of the η_{ov} and η_{ad} for a range of coolant mass flow rates from 0.088kg/sm^2 to 1.47kg/sm^2. The corresponding values in this range of G in terms of the blowing ratio, M ranges from 0.2 to 3.26. The η_{ad} contours in Fig.10 for the values of G between 0.088 – 0.35kg/sm^2, shows that the coolant air is concentrated along the jet trajectories in the holes centreline, indicating attached film cooling but with little lateral spread. Also, evident in Fig. 10 is the deterioration of the coolant air concentrations at the holes centreline with the increases in the G above 0.35 kg/sm^2. This indicates an increasing coolant jet lift-off with increasing G higher than 0.35 kg/sm^2 and consequently poor film cooling protection for the test plate hot surface. Mainly, this is the reason for the ineffectiveness of using more coolant mass flow than 0.35 kg/sm^2 in achieving better overall cooling.

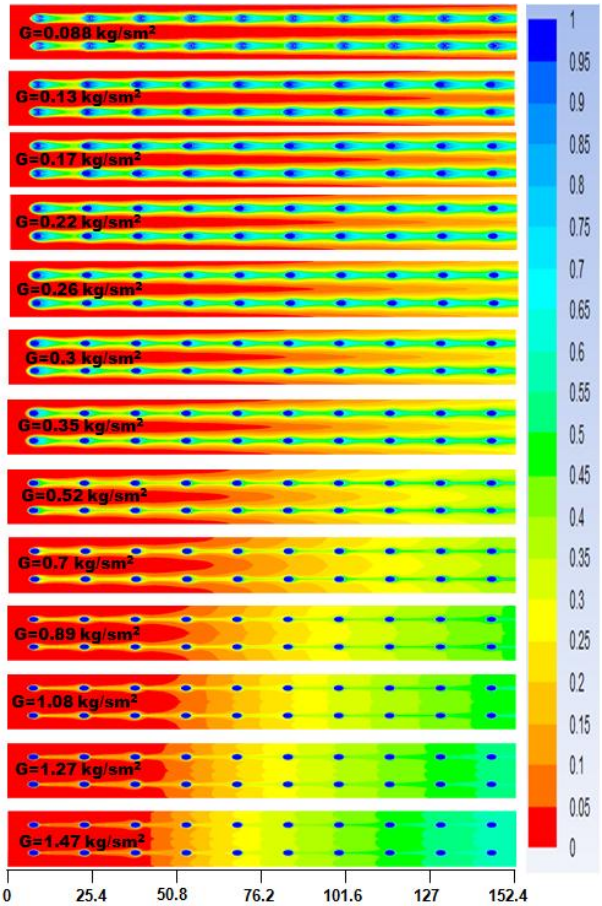

Fig. 10 Contours of the test surface spatial adiabatic film cooling effectiveness

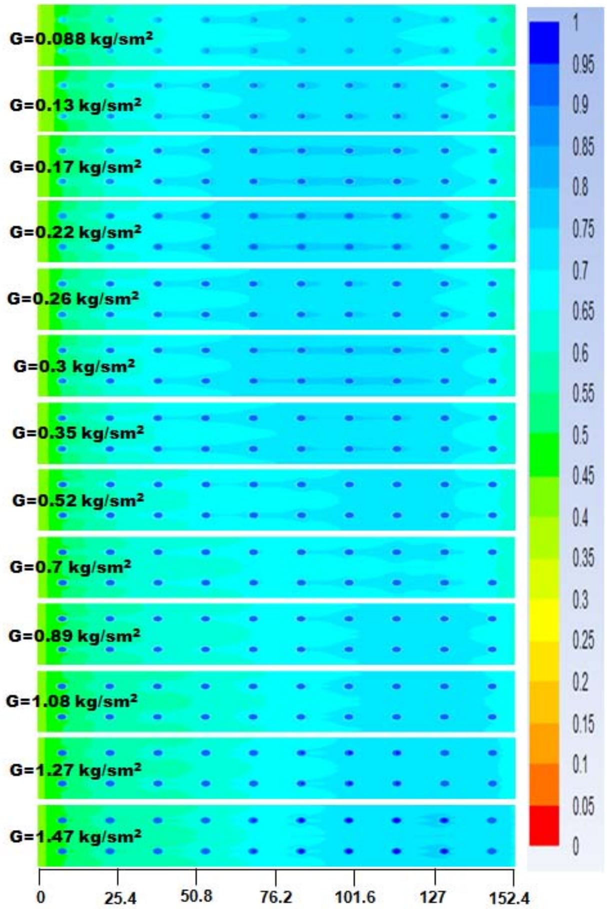

Fig. 11 Contours of the test surface spatial overall cooling effectiveness

The distributions of the η_{ov} contours for various G values are shown in Fig. 11. This shows that the wall was predicted to be relatively uniformly cooled in the lateral direction with a slow improvement in the cooling with axial distance. This is not surprising as the average value of the Biot numbers for all the test cases is 0.07. Similarly, Gustafsson et al. [40] found smoother surface temperature profiles for a cooled steel effusion plate than the adiabatic Teflon effusion plate. However, in the present study, there was some evidence of slightly higher overall cooling effectiveness directly in line with the effusion holes at low G and M. This was due to the better film cooling in this region, as shown in Fig. 10.

For G > 0.35 kg/sm^2 there was no significant improvement in the surface distribution of the cooling effectiveness. This illustrates the ineffectiveness of increasing the coolant mass flow when the coolant jets detached from the wall surface and penetrates into the crossflow.

CONCLUSIONS

1. Conjugate heat transfer CFD predictions of the overall cooling effectiveness for effusion cooled walls have been successfully achieved. There was good agreement with experimental measurements of the overall cooling effectiveness.

2. The addition of a tracer gas into the effusion film cooling flow in the computational model enables the scalar mixing of the coolant jet with the crossflow to be separate from the temperatures in the boundary layer, which are influenced by heat transfer to the wall.

3. The heat transfer within the wall was predicted to be very significant. The surface heat transfer as the coolant accelerates into the hole was of a similar magnitude to the internal hole cooling at the centre of the test plate.

4. For X/D = 4.66 and N = 4306/m^2, the predictions and experiments showed that there was little improvement in the overall cooling effectiveness for G>0.035 kg/sm^2 or M>0.8. This corresponds with the flow rate at which the coolant jets lifted off the wall and penetrated and stirred the film cooling layer. The additional wall internal cooling by the increased mass flow did not compensate for the deterioration in the film cooling caused by the increasing velocity of the coolant jet stirring effect.

5. The overall wall cooling effectiveness was predicted to be much more uniform than the adiabatic cooling effectiveness due to the internal heat conduction within the metal wall.

6. The conjugate heat transfer CFD procedures used here are in sufficiently good agreement with the experimental data for them to be used to predict the influence of effusion cooling hole array design.

ACKNOWLEDGEMENTS

Habeeb Idowu Oguntade wishes to express his profound gratitude to the Government of Lagos-State in Nigeria under the leadership of Governor Babatunde Raji Fashola (SAN) for a PhD scholarship. The experimental work was supported by four EPSRC research grants.

NOMENCLATURE

A = Area of the coolant hole, m^2
C = mass fraction of the tracer gas
D = Injection hole diameter, m
DR = Density Ratio, ρ_j/ρ_g
VR = Velocity Ratio, u_j/u_g
G = Coolant mass flow rate per unit surface area, kg/sm^2
L = Hole length, m
L/D= Ratio of the injection hole length to hole diameter
LE = Leading edge
M = Blowing ratio = $\rho_j u_j / \rho_g u_g$
N = Number of holes per unit surface area, m^{-2}
T = Temperature, K
Tu = turbulence intensity
u = Mean velocity, m/s
X = Hole pitch, m
X^2 = Surface area cooled by an individual film cooling hole, m^2
x, y, z= Cartesian coordinate system
X/D = Hole pitch to diameter ratio
y+ = Normalized distance from the wall = $\rho u_\tau y / \mu$
where the friction velocity, $u_\tau = \sqrt{\tau_w / \rho}$
ρ = Density, kg/m^3
α = Film cooling hole injection angle
η_{ov} = Overall cooling effectiveness = $(T_g - T_w)/(T_g - T_c)$
η_{ad} =Adiabatic cooling effectiveness = $(C_g - C_w)/(C_g - C_c)$

SUBSCRIPTS

ad = adiabatic
c = plenum coolant air
g = hot gas
j = jet
ov = overall
w = wall surface

REFERENCES

[1] Je-Chin Han, Sandip Dutta, and Srinath V. Ekkad, 2000, "Gas Turbine Heat Transfer and Cooling Technology", New York; Taylor and Francis.
[2] Andrews, G.E., Asere, A.A. and Mkpadi, M.C., 1984, "Transpiration and Full Coverage Discrete Hole Film Cooling", Proceedings of the 11th IChemE Annual Research Meeting.
[3] Andrews, G.E. and Asere, A.A., 1984, "Transpiration Cooling of Gas Turbine Combustion Chamber Walls", First UK National Heat Transfer Conference, IChemE Symposium Series No. 86, vol.2, pp.1047-1056.
[4] Andrews, G.E., Asere, A.A., Mkpadi, M.C. and Tirmahi, A., 1986, "Transpiration Cooling: Contribution of Film Cooling To The Overall Cooling Effectiveness", ASME Paper 86-GT-136.
[5] Andrews, G.E., Asere, A.A., Hussain, C.I. and Mkpadi, M.C., 1985, "Transpiration and Impingement/Effusion Cooling of Gas Turbine Combustion Chambers", Proc. Seventh ISABE, Beijing, AIAA, pp. 794-803.
[6] Esgar, J.B., 1971, "Turbine Cooling – Its Limitations and its Future", AGARD-CP-73-71, High Temperature Turbines, Paper 14.
[7] Andrews, G.E. and Kim, M.N., 2001, "The Influence of Film Cooling On Emissions for a Low Radial Swirler Gas Turbine Combustor", ASME Paper 2001-GT-71.
[8] Wieghardt, K., 1946, "Hot-Air Discharge for De-Icing" AAF Transaction, report no. F-TS-919-RE
[9] Goldstein, R.J., Eckert, E.R.G., and Burggraf, F., 1974, "Effects of Hole Geometry and Density on Three-Dimensional Film Cooling" Int. Journal of Heat Mass Transfer Vol. 17, pp. 595-607.
[10] Pederson, D.R., Eckert, E.R.G. and Goldstein, R.J., 1977, "Film Cooling with Large Density Differences Between the Mainstream and the Secondary Fluid Measured by the Heat-Mass Transfer Analogy", Trans. ASME, J. Heat Transfer, Vol. 99 p. 620-627.
[11] Pietrzyk, J.R., Bogard, D.G. and Crawford, M.E., 1989, "Effects of Density Ratio on the Hydrodynamics of Film Cooling" ASME Paper 89-GT-175.
[12] Sinha, A.K., Bogard, D.G. and Crawford, M.E., 1990, "Film Cooling Effectiveness Downstream of a Single Row of Holes with Variable Density Ratio", ASME Paper 90-GT-42.
[13] Kohli, A., and Bogard D.G., 1997, "Adiabatic effectiveness, thermal fields, and velocity field for film cooling with large angle injection", J. of Turbomachinery Vol.119, pp.352-356.

[14] Bacci, A., and Facchini, B., 2007, "Turbulence modelling for the numerical simulations of film and effusion cooling flows", ASME GT2007-27182.

[15] Oguntade H.I., Andrews, G.E., Alan, B., Ingham, D., and Pourkashanian, M., 2010, "CFD Predictions of Single Row Film Cooling With Inclined Holes: Influence of Hole Outlet Geometry", Proc. of ASME Turbo Expo 2010: Power for Land, Sea and Air, ASME GT-2010-22308.

[16] Andrews, G.E. and Mkpadi, M.C., 1983, "Full Coverage Discrete Hole Wall Cooling - Discharge Coefficients", ASME 83-GT-192. Also in Journal of Engineering for Power, Vol.106, pp.183-192 (1984).

[17] Andrews, G.E., Gupta, M.L. and Mkpadi, M.C., 1984, "Combined Radiative and Convective Heat Transfer In An Enclosure", First UK National Heat Transfer Conference, IChemE Symposium Series No. 86, Vol.2, pp. 979-988.

[18] Andrews, G.E., Gupta, M.L. and Mkpadi, M.C., 1985, "Full Coverage Discrete Hole Film Cooling: Cooling Effectiveness", International Journal of Turbo and Jet Engines, Vol.2, pp.199-212.

[19] Andrews, G.E., Asere, A.A., Gupta, M.L. and Mkpadi, M.C., 1985, "Full Coverage Discrete Hole Film Cooling: The Influence of Hole Size", ASME Paper 85-GT-53. Also in the International Journal of Turbo and Jet Engines, Vol.2, pp.213-225 (1985).

[20] Andrews, G.E., Asere, A.A., Gupta, MX. Mkpadi, M.C. and Tirmahi A., 1990, "Full Coverage Discrete Hole Film Cooling: The Influence of the Number of Holes and Pressure Loss", ASME Paper 90-GT-61.

[21] Andrews, G.E., Asere, A.A., Gupta, M.L. and Mkpadi, M.C., 1990, "Effusion Cooling: The Influence of the Number of Holes", Proceedings of the Institution of Mechanical Engineers, Vol.204, Part A, Journal of Power and Energy, pp.175-182 (1990).

[22] Bazdidi-Tehrani, F. and Andrews, G.E., 1993, "Full Coverage Discrete Hole Film Cooling: Investigation of the Effect of Variable Density Ratio", ASME COGEN TURBO POWER '93. Also in ASME Journal of Heat Transfer (1994).

[23] Andrews, G.E., Khalifa, I.M., Asere, A.A. and Bazdidi-Tehrani, F., 1995, "Full Coverage Effusion Film Cooling With Inclined Holes", ASME Paper 95-GT-274.

[24] Bazdidi-Tehrani, F. and Andrews, G.E., 1996, "Full Coverage Discrete Hole Film Cooling: Investigation of the Effect of Variable Density Ratio (Part I)", ASME Paper 96-GT-264.

[25] Bazdidi-Tehrani, F. And Andrews, G.E., 1997, "Full Coverage Discrete Hole Film Cooling Investigations of The Effect of Variable Density Ratio (Part II)", ASME Paper 97-GT-341.

[26] Andrews, G.E., Alikhanizadeh, M., Asere, A.A, Hussain, C.I., Koshkbar Azari, M.S. and Mkpadi, M.C., 1986, "Small Diameter Film Cooling Holes: Wall Convective Heat Transfer", ASME Paper 86-GT-225.

[27] Andrews, G.E. and Bazdidi-Tehrani, F., 1989, "Small Diameter Film Cooling Hole Heat Transfer: The Influence of the Number Of Holes", ASME Paper 89-GT-7.

[28] Andrews, G.E., Alikhanizadeh, M., Bazdidi Tehrani, F., Hussain, C.I. and Koshkbar Azari, M.S., 1988, "Small Diameter Film Cooling Holes: The Influence Of Hole Size And Pitch", International Journal of Turbo and Jet Engines, Vol. 5, pp. 61-73, 1988.

[29] Andrews, G.E., Bazdidi-Tehrani, F., Hussain, C.I. and Pearson, J.P., 1991, "Small Diameter Film Cooling Hole Heat Transfer: The Influence of the Hole Length", ASME Paper 91-GT-344.

[30] Andrews, G.E., Asere, A.A., Hussain, C.I. and Mkpadi, M.C., 1985, "Transpiration and Impingement/ Effusion Cooling of Gas Turbine Combustion Chambers", Proceedings of The Seventh International Symposium on Air Breathing Engines, AIAA, pp.804-812.

[31] Andrews, G.E., Asere, A.A., Hussain, C.I., Mkpadi, M.C. and Nazari, A., 1988, "Impingement/Effusion Cooling: Overall Wall Heat Transfer", ASME Paper 88-GT-290.

[32] Al-Dabagh, A.M., Andrews, G.E., Abdul-Husain, R.A.A., Husain, C.I., Nazari, A. and Wu, J., 1990, "Impingement/Effusion Cooling: The Influence of The Number of Impingement Holes and Pressure Loss on the Heat Transfer Coefficient", J. Turbomachinery, Vol.112, pp.467-476.

[33] Andrews, G.E., Al-Dabagh, A.M., Asere, A.A., Bazdidi-Tehrani, F., Mkpadi, M.C. and Nazari, A., 1992, "Impingement/Effusion Cooling", AGARD Propulsion and Energetics Panel, 80th Symposium on Heat Transfer and Cooling in Gas Turbines, Turkey. AGARD Conference Proceedings 527, pp.30.1-30.10.

[34] Andrews, G.E. and Nazari, A., 1999, "Impingement/Effusion Cooling: Influence of The Number of Holes On The Cooling Effectiveness For An Impingement X/D Of 10.5 and Effusion X/D Of 7.0", Proceedings of the International Gas Turbine Congress, pp.639-646.

[35] Jung, E.Y., Lee, D.H., Oh, S.H., Kim, M.K., and Cho, H.H., 2010, " Total Cooling Effectiveness On A Staggered Full-Coverage Film Cooling Plate With Impinging Jet", ASME GT2010-23725.

[36] Oh, S.H., Lee, D.H., Kim, M.K., Kim, M.Y., and Cho, H.H., 2008, "Enhanced Cooling

Effectiveness In Full-Coverage Film Cooling System With Impingement Jets", ASME GT2008-50784.
[37] Crawford, M.E., Choe, H., Kays, W.M., and Moffat, R.J., 1976, "Full-Coverage Film Cooling Heat Transfer Study- Summary of Data for Normal-Hole Injection and 30^0 Slant-Hole Injection", Contractor Report CR-2648, NASA.
[38] Jeromin, A., Eichler, C., Noll, B., and Aigner, M., 2008, "Full 3D Conjugate Heat Transfer Simulation and Heat Coefficient Prediction For The Effusion-Cooled Wall of a Gas Turbine Combustor", ASME GT2008-50422.
[39] Harrington, M., McWaters, M., Bogard, D., Lemmon, C., and Thole, K. A., 2001, "Full-Coverage Film Cooling with Short Normal Injection Holes," J. of Turbomachinery Vol. 123, pp. 798–805.
[40] K.M. Bernhard Gustafsson, T. Gunnar Johansson, "An experimental study of surface temperature distribution on effusion-cooled plates", Journal of Engineering for Gas Turbines and Power, Vol. 123, pp. 308–316.
[41] Scrittore, J. J. Thole, K. A., and Burd, S. W., 2001, "Investigation of Velocity Profiles For Effusion Cooling of a Combustor Liner," J. of Turbomachinery Vol. 123, pp. 798–805.